Electrochimica Acta 55 (2010) 620–631

Contents lists available at ScienceDirect

Electrochimica Acta

journal homepage: www.elsevier.com/locate/electacta

Electrochemical and surface analytical studies of the self-assembled monolayer of 5-methoxy-2-(octadecylthio)benzimidazole in corrosion protection of copper

B.V. Appa Rao[a,*], Md. Yakub Iqbal[a], B. Sreedhar[b]

[a] Department of Chemistry, National Institute of Technology, Warangal 506004, Andhra Pradesh, India
[b] Inorganic & Physical Chemistry Division, Indian Institute of Chemical Technology, Hyderabad 500007, India

ARTICLE INFO

Article history:
Received 12 April 2009
Received in revised form 3 September 2009
Accepted 4 September 2009
Available online 9 September 2009

Keywords:
Impedance
EQCN
SAM
XPS
Copper

ABSTRACT

5-Methoxy-2-(octadecylthio)benzimidazole (MOTBI) monolayer was self-assembled on fresh copper surface obtained after etching with nitric acid at ambient temperature. The optimum conditions for formation of self-assembled monolayer (SAM) were established using impedance studies. The optimum conditions are methanol as solvent, 10 mM concentration of the organic molecule and an immersion period of 24 h. The MOTBI SAM on copper surface was characterized by contact angle measurements, X-ray photoelectron spectroscopy and reflection absorption FTIR spectroscopy and it is inferred that chemisorption of MOTBI on copper surface is through nitrogen. Corrosion protection ability of MOTBI SAM was evaluated in aqueous NaCl solution using impedance, electrochemical quartz crystal nanobalance, potentiodynamic polarization and weight-loss studies. While bare copper showed a charge-transfer resistance (R_{ct}) value of 1.89 kΩ cm^2 in 0.20 M NaCl aqueous environment, the R_{ct} value for SAM covered copper surface is 123.4 kΩ cm^2. The MOTBI SAM on copper afforded corrosion inhibition efficiency of 98–99% in NaCl solution in the concentration range and in the temperature range studied. The SAM functions as a cathodic inhibitor. Quantum chemical calculations showed that MOTBI has relatively small ΔE between HOMO and LUMO and large negative charge in its benzimidazole ring, which facilitate formation of a polymeric [Cu^+-MOTBI] complex on copper surface.

1. Introduction

Copper metal is widely used in microelectronic packaging [1]. The advantages of copper over aluminium are lower resistance and higher reliability [2]. Wire bonding is the commonly used method to connect the chip to the outside world in microelectronic packaging [3]. The advantages of copper have rapidly established itself as one of the main materials for the wire bonding as an alternative to gold in microelectronic packaging. Reduced cost, enhanced device speed, and improved reliability of a monometallic system are the primary drivers of the emergence of Cu–Cu processes [3]. Ho et al. extensively carried out studies on copper wire bonding to copper bond pads [2]. But copper is an active metal, which readily undergoes oxidation in air. Oxidation of copper is considered a serious reliability problem in microelectronic packaging. Therefore corrosion inhibition of copper is becoming very important in microelectronic packaging. Copper wire bonding is normally formed by a copper ball onto a copper based bond pad in microelectronic package. Copper bond pad oxidizes readily and the oxide continues to grow in thickness. As oxidation of copper bond pad is the main issue, this is being looked into when it is still a wafer [2]. Solder interconnection is one of the most common methods used for the joining of components to printed circuit boards (PCBs) in electronics industry [4]. During soldering, it is a common practice to use a flux to remove any oxide layers or other contaminants from the surfaces of the metals to be joined [4]. Most fluxes consist of organic or inorganic acids, which at the high temperature of the soldering process chemically remove the oxides exposing the clean, reactive metal surface. The flux residue containing ionic contaminants such as copper and tin ions and unused acidic components, which if left on the circuit board can cause corrosion of joints and electrical shorting due to electromigration [4].

Self-assembled monolayers (SAMs) are dense and ordered monolayers [5], which act as effective barriers and protect copper against corrosion [6]. Laibinis and Whitesides reported that alkanethiols adsorbed on copper surface form densely packed SAMs, which were found to be effective inhibitors of copper corrosion in air [6]. Feng et al. reported the corrosion protection of self-assembled alkanethiol monolayer on copper in a 0.5 M NaCl solution [7]. Aramaki and co-workers reported that the maximum efficiency of the SAM of octadecanethiol for protection of corrosion of copper in 0.5 M Na_2SO_4 solution was 80.3% [8]. Quan et al. studied the corrosion protection ability of the SAMs of schiff bases

* Corresponding author. Tel.: +91 870 2462652; fax: +91 870 2459547.
E-mail addresses: boyapativapparao@rediffmail.com, chemysri@yahoo.com (B.V. Appa Rao), yakub_iqbal@yahoo.com (Md.Y. Iqbal).

0013-4686/$ – see front matter © 2009 Elsevier Ltd. All rights reserved.
doi:10.1016/j.electacta.2009.09.007

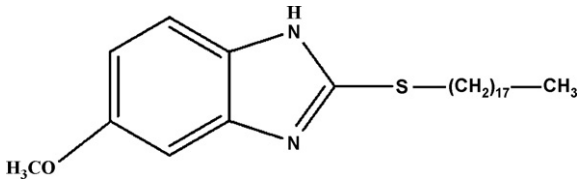

Fig. 1. Structure of 5-methoxy-2-(octadecylthio)benzimidazole.

on copper surfaces [9,10]. Protection of copper bond pad surface from oxidation is the key issue in wire bonding process. Corrosion protection of copper bond pad can be achieved by formation of an organic monolayer on the surface of the pad in a suitable solvent by self-assembly process. SAM protects the copper bond pad surface until it is removed by the ultrasonic energy during wire bonding. The mechanism of formation of the ball bond involves the removal of the SAM by the ultrasonic energy in the first step and then the formation of welded interface in between the deformed ball and the bond pad [2]. Liu and Hutt studied [4] self-assembled monolayer of octadecanethiol as a preservative to enable fluxless soldering of copper substrates. Preservation of copper surfaces to enable fluxless soldering involves the etching of the copper surface in the first step to remove the native oxide, followed by the application of an organic monolayer that acts as a barrier to the diffusion of oxygen, enabling the material to be stored in air for a longer period. During the soldering process, the coating is displaced by the temperature rise and by the molten solder, revealing an oxide free active surface that can be protected from re-oxidation by the use of an inert atmosphere [4]. SAMs are utilized to prevent the electromigration and surface scattering of copper atoms while minimizing the resistance of the interconnect lines [11]. Electromigration and surface diffusion are prevented because the organic layer is covalently bound to the metal atoms in the metal interface. Additionally the organic molecules in the organic layer are relatively large and will help hold the metal atoms in place because it is virtually impossible for metal atoms to migrate when covalently bound to large organic molecules.

So far no comprehensive studies have been reported in the literature on corrosion protection of SAMs formed by heterocyclic organic compounds containing long alkyl chains. Therefore it was of interest to investigate the optimum conditions for the formation of SAM of 5-methoxy-2-(octadecylthio)benzimidazole (MOTBI), the corrosion protection efficiency of MOTBI SAM and the mechanistic aspects of corrosion protection by this SAM. The reasons for choosing the MOTBI compound in the present study for the formation of SAM on copper surface are as follows. The structure of MOTBI is shown in Fig. 1. MOTBI consists of four active sites namely two nitrogens, one sulfur and one oxygen for chemisorption and chelation with copper ions to form a protective film on copper surface. It also consists of a long hydrocarbon chain to make the film hydrophobic. Imidazoles are known to be non-toxic or less toxic inhibitors as alternatives to benzotriazoles for corrosion inhibition of copper [12]. It is relevant to mention the reports in the literature on imidazoles, benzimidazole and mercaptobenzimidazole (MBI) as corrosion inhibitors for copper in a variety of environments. Stupnisek-Lisac et al. [13] reported the evaluation of non-toxic corrosion inhibitors for copper in dilute sulfuric acid. They found a high inhibition efficiency of 93% by adding a phenyl ring to the imidazole structure. The efficiency of non-toxic imidazole derivatives to inhibit corrosion of copper in sodium chloride solution was reported by Otmac and Stupnisek-Lisac [14], who found that the imidazoles with phenyl ring have better inhibiting properties than others. Lee [15] reported the inhibiting effect of imidazole on copper corrosion in 1 M HNO_3 solution and attributed it to the formation of a protective film of Cu–imidazole complex. Stupnisek-Lisac et al. [16] reported that 5-hydroxy methyl-4-methylimidazole and 5-hydroxy methyl-4-methylimidazole hydrochloride showed significant atmospheric corrosion protection of copper on printed circuit boards.

Zhang et al. [17] studied the synergistic effect of 2-mercaptobenzimidazole and KI on copper corrosion inhibition in aerated 0.5 M sulfuric acid solution. They attributed the synergistic effect to the adsorption of iodide ions on the copper surface, which then facilitated the adsorption of protonated MBI and formation of a protective film of (Cu^+-MBI) complex. In the absence of iodide ion, the inhibition efficiency of MBI was found to be somewhat less. Zhang et al. [18] reported that 2-mercaptobenzimidazole was found to be the most effective corrosion inhibitor among benzotriazole, 2-mercaptobenzoxazole and 2-mercaptobenzimidazole to inhibit corrosion of copper in 0.5 M HCl. Larabi et al. [19] reported that 2-mercapto-1-methylimidazole inhibited corrosion of copper in dilute hydrochloric acid environment. Effect of adsorption of some azoles on copper passivation in alkaline medium has been reported by Subramanian and Lakshminarayanan [20]. The relative inhibition efficiencies have been reported to be in the order, mercaptobenzothiazole > benzimidazole ≈ mercaptobenzimidazole > benzotriazole ≈ imidazole. It was also reported that more than 95% coverage is complete in case of all the molecules. Xue et al. [21] investigated the chemisorption of 2-mercaptobenzimidazole onto a chemically cleaned surface of metallic copper from its ethanol solution by surface enhanced Raman scattering, X-ray-induced Auger spectroscopy and infrared spectroscopy. They inferred that MBI reacts directly with metallic copper to form 2-mercaptobenzimidazolates, which covered the surface with a polymeric film. Xue et al. [22] showed that the film formed on copper surface by MBI from ethanol solution is more stable and has better anti-corrosive property than the corresponding film from an oxidized copper surface. Carron et al. [23] assessed the inhibition of copper corrosion by a mixture of polybenzimidazole and mercaptobenzimidazole by *in situ* SERS and cyclic voltammetry. They concluded that a very compact protective layer covering the entire surface is formed by the mixture. MBI was reported to show 20% more inhibition effect on copper corrosion in aerated sulfuric acid solution in comparison to benzotriazole [12].

From the above studies reported in the literature it is evident that mercaptobenzimidazole is a good candidate for corrosion protection of copper in a variety of environments. It was interpreted [21–23] that mercaptobenzimidazole forms a protective film through sulfur, forming copper mercaptobenzimidazolate complex. The hydrogen present in the mercapto group is easily replaced in the process. But, in the case of MOTBI, the complexation is expected to be through nitrogen with a high negative charge and not through sulfur as sulfur is attached to a long alkyl chain. The long hydrocarbon chain, however, can provide the hydrophobic nature to the SAM. Moreover, the detailed and systematic studies on the optimum conditions for the formation of SAM, characterization of SAM and corrosion protection ability of the SAM formed by either MBI or MOTBI using several experimental techniques have not been reported so far in the literature and hence the need for the present study. Then, a question arises as to how the SAM formed by MOTBI is different from the SAM formed by alkanethiols, for which systematic studies are available in the literature. In the case of MOTBI, the participating nitrogens in complexation with cuprous ions are members of the extended conjugated system in which nine atoms can share the charge by mesomerism. Hence the energy of the complex formed between MOTBI and Cu^+ is expected to be much smaller than the energy of the complex formed between Cu^+ and alkanethiols. Therefore, the stability of the complex between MOTBI and Cu^+ is expected to be much greater than the stability of the complex formed between Cu^+ and alkanethiols. In the term

'self-assembled monolayer', monolayer usually means a complete single layer of molecules on a surface. In the present paper the term 'monolayer' is used to indicate a single layer of molecules, even if the surface coverage is not complete to an extent of 100%.

2. Experimental

2.1. Materials

MOTBI was synthesized by mixing equimolar amounts of 1-bromooctadecane and 5-methoxy-2-mercaptobenzimidazole in round-bottomed flask in the presence of a solvent mixture of N, N-dimethylformamide and anhydrous ethanol and then refluxing for 6 h [24]. All the chemicals used were A.R. grade and were purchased from Qualigens Chemicals (Pvt. Ltd.), India. Differential scanning calorimetry (DSC) and ^{1}H NMR techniques were used for characterization of MOTBI. Four hundred and thirty-two milligrams of MOTBI was dissolved in methanol to get a 10 mM solution. 1 mM, 2.5 mM and 5 mM solutions were prepared by dilution from 10 mM solution. Polycrystalline copper specimens of different dimensions were made from a copper sheet of purity 99.9%. For electrochemical impedance and potentiodynamic polarization studies, the copper specimens of the dimensions 4 cm × 1.0 cm × 0.2 cm were used and only 1 cm^2 area was exposed to the electrolyte, while the remaining area was insulated with epoxy resin. For surface analytical studies 1.0 cm × 1.0 cm × 0.2 cm specimens were used. For weight-loss studies 4.0 cm × 1.0 cm × 0.2 cm specimens were used. These specimens were polished to mirror finish using 1/0, 2/0, 3/0, 4/0 grade emery papers and alumina powder on rotating disk and then degreased with acetone. The specimens were washed with double distilled water and dried with nitrogen for 20 min. For electrochemical quartz crystal nanobalance studies copper quartz crystals of dimensions 0.20 cm^2 were used.

2.2. Formation of SAMs

Solubility of MOTBI was tested in the organic solvents such as acetone, chloroform, methanol, ethyl acetate and *n*-hexane. It was found that MOTBI is insoluble in acetone, chloroform, ethyl acetate and *n*-hexane whereas it is relatively less soluble in methanol. Therefore methanol was chosen as solvent for formation of MOTBI SAM on copper surface. To obtain a dense and stable SAM, the best immersion time was reported to be more than 20 h by Quan et al. [9] in their studies on formation of SAM of schiff base on copper. Ishibashi et al. [25] reported that in the case of alkanethiols, the SAM formed at 5 mM concentration in ethanol was found to form a protective layer on copper surface. Therefore in the present study an immersion period of 24 h and 5 mM concentration of MOTBI were fixed initially for the study of formation of SAM in methanol solvent Then, the effect of concentration of MOTBI and the effect of the variation of immersion period were studied in order to optimize the conditions for formation of SAM. The polished copper specimens were etched with 7N nitric acid for 30 s, washed with triple distilled water followed by the organic solvent as quickly as possible and then immediately immersed in different concentrations of MOTBI solution in methanol for various immersion periods.

2.3. Electrochemical studies

Electrochemical impedance studies were first carried out in order to establish the optimum conditions for the formation of protective SAM on copper surface. The impedance studies were carried out in a three-electrode cell assembly (in accordance with ASTM specifications) using an electrochemical workstation model IM6e ZAHNER elektrik, Germany. The bare copper specimen or the MOTBI SAM modified copper specimen was used as the working electrode. A platinum electrode was used as the counter electrode and the reference electrode was a silver–silver chloride electrode. Impedance measurements were carried out at the open-circuit potential in the frequency range from 60 kHz to 10 mHz and Nyquist plots were obtained. The impedance studies were also carried out in order to investigate the corrosion protection ability of the SAM in an aggressive environment viz., NaCl in the concentration range of 0.02–0.20 M, at various immersion periods (0.5–24 h) and at various temperatures (30–60 °C). Inhibition efficiencies were calculated from the impedance data. Potentiodynamic polarization studies were carried out in a three-electrode cell assembly at different concentrations (0.02–0.20 M) in NaCl environment using the same electrochemical workstation and the cell assembly used for impedance studies. The polarization curves were recorded in the potential range of −0.500 V to +0.200 V vs. Ag/AgCl at a scan rate of 1 mV/s. Correction of the curves for IR-drop compensation was not required because of the high electrical conductivity of the aggressive corrosive environments [26]. The reference electrode was kept very near to the working electrode. Electrochemical quartz crystal nanobalance system, model Elchema EQCN-700 and an AT-cut copper quartz crystal with 10 MHz nominal frequency were used in these studies. The copper quartz crystal was immersed in the MOTBI solution in ethyl acetate solvent and the mass change as a function of time was recorded during the formation of SAM on the copper crystal. The corrosion protection ability of the MOTBI SAM was also found using EQCN studies. The MOTBI modified copper quartz crystal was immersed in 0.02 M NaCl solution and the mass change was recorded as a function of time up to 24 h. A positive mass change indicates mass gain and a negative mass change indicates mass loss.

2.4. Contact angle measurements

Contact angle measurements for bare copper and copper covered with MOTBI SAM were made by sessile water drop method using a contact angle measuring system, model G10, Kruss, Germany. The measurements were carried out at about 30 °C in air.

2.5. Surface analytical techniques

FTIR measurements for bare copper and copper covered with SAM were recorded in single reflection mode using FTIR spectrometer, model Thermo-Nicolet Nexus 670 of the Thermo Electron Corporation, USA in the spectral range of 400–4000 cm^{-1} with a resolution of 4 cm^{-1}. This FTIR instrument has KBr window and XT-KBr beam splitter and lowest possible wave number is 400 cm^{-1}. Bare copper and MOTBI SAM covered copper specimens were mounted on the reflection accessory and the plane polarized light was incident at a grazing angle of 85° from the surface normal. The sample compartment was continuously purged with nitrogen during the measurement. The surface analysis of bare copper and MOTBI SAM covered copper was carried out using the X-ray photoelectron spectrometer, ESCA Kratos model AXIS-165, with Mg Kα radiation (1253.6 eV) and energy resolution of 0.1 eV. Computer deconvolution was applied to detect the elemental peaks of copper, oxygen, carbon, nitrogen and sulfur present in the SAM. XPS studies were also used to analyze the nature of the surface films in the presence of a corrosive environment, 0.02 M NaCl.

2.6. Weight-loss studies

The bare copper specimens and the copper specimens covered with SAM were immersed in 0.02 M NaCl solution for a period of 3 days. The weights of the specimens before and after immersion were recorded by using an electronic balance with a readability of

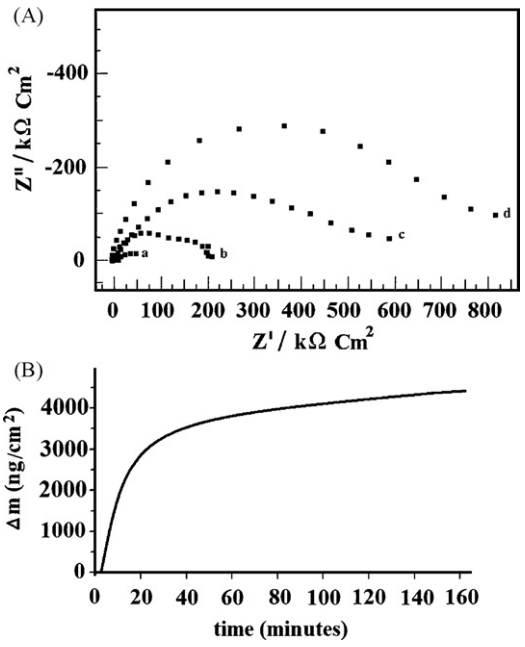

Fig. 2. (A) Nyquist plots of copper with SAM formed in 10 mM MOTBI at different immersion periods: a, 3 h; b, 6 h; c, 12 h; d, 24 h (environment: aqueous 300 ppm chloride). (B) Mass change vs. time curve during formation of SAM on copper quartz crystal in the presence of MOTBI in methanol.

0.01 mg. From the weight-loss data, the corrosion rates and inhibition efficiencies were calculated.

2.7. Quantum chemical calculations

Quantum chemical calculations were carried out using semi-empirical AM1 molecular orbital method in the MOPAC program using Chem3D Ultra Molecular Modelling and Analysis software 8.0 version. E_{HOMO}, E_{LUMO}, ΔE, net atomic charges on each of the elements of MOTBI and the total ring charge were obtained from these calculations.

3. Results and discussion

3.1. Optimum conditions for formation of MOTBI SAM

Nyquist plots for copper covered with SAM within a concentration range of 1–10 mM of MOTBI are obtained at an immersion period of 24 h. It is found that the R_{ct} value is much higher in the case of SAM formed from 10 mM concentration of MOTBI, when compared with lower concentrations. For example, R_{ct} value at 10 mM concentration of MOTBI is 723.1 kΩ cm^2. Therefore 10 mM was chosen as the optimum concentration for formation of dense and protective SAM. By fixing the concentration of the MOTBI solution as 10 mM, Nyquist plots are obtained at different immersion periods in the range of 3–24 h in 8.4×10^{-3} M NaCl environment and shown in Fig. 2A. It may be noted that at 3 h immersion period, R_{ct} value is 23.0 kΩ cm^2 and at 24 h immersion period, R_{ct} value is increased to a very large value of 723.1 kΩ cm^2.

Electrochemical quartz crystal nanobalance (EQCN) is capable of detecting mass changes in the nanoscale range. The oscillation frequency of a quartz crystal is highly sensitive to the minute mass changes at the crystal surface. One face of the crystal is modified to function as the working electrode and changes of the electrode mass are continuously monitored [27,28]. Fig. 2B shows the mass change vs. time plot obtained from EQCN experiment. The curve represents the change of mass on the copper quartz crystal surface as a function of time. The curve shows an initial increase in mass in the first 40 min followed by a tendency towards saturation with further increase in time up to 160 min. The increase of mass is due to the formation of monolayer of MOTBI on the copper surface. It is known that the formation of the self-assembled monolayer on copper surface occurs in two steps [29]. In the first step MOTBI adsorbs on the copper surface, and in the second step, it rearranges to form a monolayer. Obviously the first step involving chemisorption takes relatively less time and the second step involving the rearrangement of the organic molecules in the SAM takes relatively longer time.

3.2. Characterization of MOTBI SAM

3.2.1. Contact angle measurements

The degree of hydrophobicity of MOTBI SAM is characterized by the contact angle measurement of a sessile water drop on the copper surface covered with SAM. The contact angle values for bare copper and SAM covered copper are found to be 78° and 91° respectively. The contact angle value for the MOTBI SAM covered copper surface indicates the hydrophobic nature of the self-assembled monolayer, which in turn provides a barrier against corrosive species from attacking the underlying copper substrate. It is worth mentioning that the contact angle values reported in the literature for the SAMs of hexadecane thiol [30], octadecanoyl hydroxamic acid [31], benzene thiol and 4-amino benzene thiol [32] on copper surface are 120°, 108°, 100° and 95° respectively. From these values it can be inferred that the degree of hydrophobicity is higher in the case of SAMs formed by the molecules having aliphatic alkyl chain. The degree of hydrophobicity of MOTBI SAM is comparable to that of the SAM formed by 4-amino benzene thiol.

3.2.2. X-ray photoelectron spectroscopic studies

In the bare copper XPS spectrum, Cu $2p_{3/2}$, Cu $2p_{1/2}$, C 1s and O 1s peaks are detected. The computer deconvolution spectra for copper, carbon and oxygen are shown in Fig. 3A–C respectively. The Cu $2p_{3/2}$ peak at a binding energy of 932.6 eV and the Cu $2p_{1/2}$ peak at 952.4 eV can be attributed to Cu (I) [5]. The C 1s electron binding energy at 285 eV corresponds to contaminant carbon, which is likely due to cracking of vacuum oil used in the XPS instrument [33]. The O 1s peak observed at 531.1 eV is due to formation of Cu_2O on the copper surface [34,35], which is formed during the interval between polishing of the copper surface and the XPS analysis.

The XPS spectrum of MOTBI SAM covered copper surface shows peaks corresponding to Cu $2p_{3/2}$, Cu $2p_{1/2}$, O 1s, C 1s, N 1s, and S 2p. The computer deconvolution spectra for copper, oxygen, carbon, nitrogen and sulfur are shown in Fig. 4A–E respectively. Cu 2p spectrum shows peaks due to Cu $2p_{3/2}$ and Cu $2p_{1/2}$ at 932.9 eV and 952.6 eV respectively, which are due to the initial oxidation of copper surface to Cu_2O during SAM formation. C 1s shows two peaks, one at 284.6 eV and the other at 285.3 eV. The C 1s peak at 284.5 eV arises due to the presence of 18 carbon atoms in the alkyl chain of MOTBI [36,37]. The C 1s peak at 285.3 eV is due to the carbon present in the aromatic ring of MOTBI. The ratio of the intensities of the C 1s peak to the Cu $2p_{3/2}$ peak in the spectrum of SAM modified copper is more than 19 times higher than the corresponding ratio of intensities observed in the spectrum of bare copper. This result infers the presence of SAM of the organic molecule with a long hydrocarbon chain on copper surface. The O 1s spectrum shows two peaks. The peak at 531.4 eV is due to formation of Cu_2O on the copper surface during SAM formation. The existence of oxygen in the SAM shows that the oxygen dissolved in the solution has taken part in the self-assembly process, by oxidizing the copper surface to Cu_2O [5]. The second peak at 532.8 eV is due to the presence of oxygen in MOTBI molecule itself. N 1s spectrum also shows two peaks, one at 398.9 eV and the other at 400.2 eV, which are due to

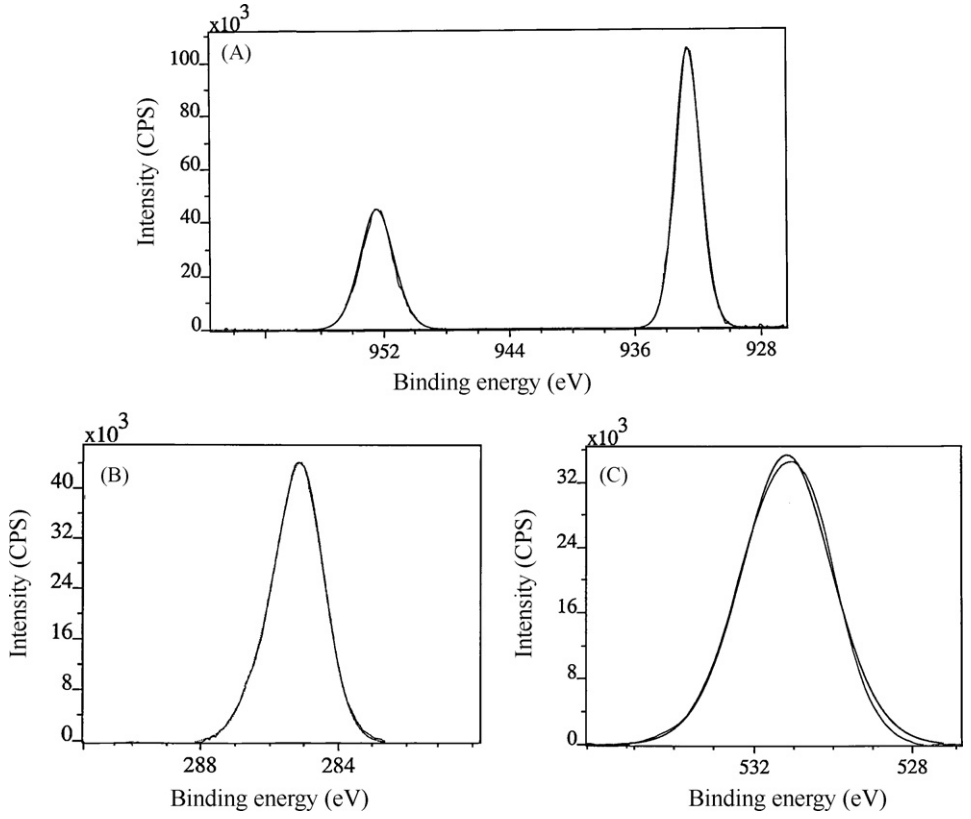

Fig. 3. XPS deconvolution spectra of different elements present on the surface of the bare copper (A, Cu 2p; B, C 1s; C, O 1s).

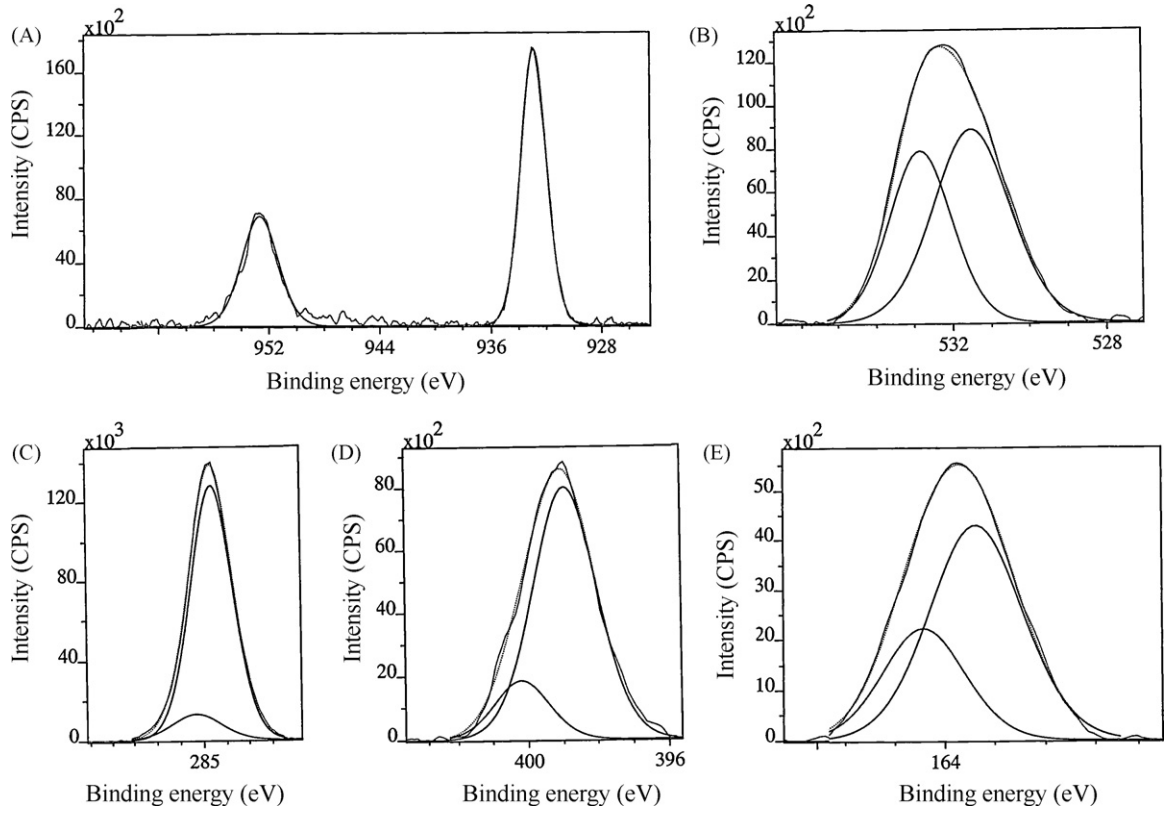

Fig. 4. XPS deconvolution spectra of different elements present on the surface of the copper covered with MOTBI SAM (A, Cu 2p; B, O 1s; C, C 1s; D, N 1s; E, S 2p).

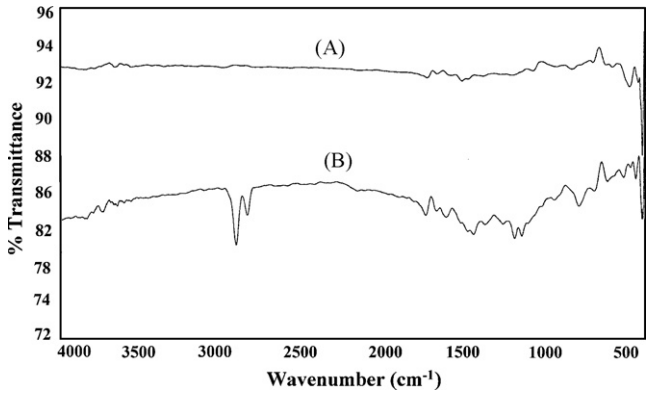

Fig. 5. Reflection absorption FTIR spectrum of (A) bare copper and (B) copper covered with MOTBI SAM.

the presence of two nitrogen atoms in MOTBI in different chemical environments. The characteristic binding energy of the elemental nitrogen is reported as 398.0 eV in the literature [38]. The shift of N 1s binding energy from elemental binding energy indicates that the two nitrogen atoms present in MOTBI play a vital role in complex formation between copper and MOTBI [33]. S 2p spectrum shows two peaks at 163.3 eV and 164.4 eV, which are due to S $2p_{3/2}$ and S $2p_{1/2}$ components respectively. There is a separation of 1.1 eV between the two peaks. In the literature when SAM formation was done through a thiolate group namely RS^-, the two peaks due to S $2p_{3/2}$ and S $2p_{1/2}$ were reported at 162.5 eV and 163.7 eV respectively, with a separation of 1.2 eV [6,32]. It must be noted that in the present study in the case of MOTBI SAM sulfur is not present as thiolate but as sulfur with a lone pair of electrons and hence the observed slightly higher binding energy values of the two S 2p peaks.

3.2.3. FTIR reflection absorption studies

FTIR reflection absorption spectra for bare copper and the copper covered with MOTBI SAM are shown in Fig. 5A and B respectively. For bare copper, the spectrum shows a peak at 489.5 cm^{-1} which is assigned to copper oxide on the surface [39]. Mekhalif et al. [40] studied the comparative assessment of *n*-dodecanethiol and *n*-dodecaneselenol monolayers on electroplated copper. In their infrared reflection absorption study they interpreted the two bands at 2922 cm^{-1} and 2851 cm^{-1} to the asymmetric CH_2 and symmetric CH_2 modes respectively. Yoshida and Ishida [41] studied FTIR reflection absorption spectrum of undecyl-imidazole on copper surface. They obtained two bands at 2853 cm^{-1} and 2925 cm^{-1} and interpreted them due to CH_2 symmetric stretching mode and CH_2 asymmetric stretching mode respectively. Laibinis et al. [42] compared the structural and wetting properties of self-assembled monolayers of *n*-alkanethiols on the coinage metal surfaces, Cu, Ag and Au. They have investigated the film structure and molecular orientation by IR vibrational spectroscopy. In their study, the peaks at 2925 cm^{-1} and 2850 cm^{-1} were assigned to CH_2 asymmetric stretching and CH_2 symmetric stretching modes respectively. Silverstein and Webster [43] mentioned that in methylene groups, the asymmetrical stretching and symmetrical stretching occur at 2926 cm^{-1} and 2853 cm^{-1} respectively. In the present study the reflection absorption FTIR spectrum exhibited two bands, one at 2851 cm^{-1} and the other at 2920 cm^{-1}. These two bands may be interpreted due to CH_2 symmetric stretch and CH_2 asymmetric stretch modes respectively. Thus there is a clear evidence of aliphatic hydrocarbon chain present in the SAM formed on copper surface. The FTIR reflection absorption spectrum of MOTBI SAM covered copper also shows the appearance of C=C stretching band at 1625 cm^{-1}, C=N stretching band at 1456 cm^{-1}, C–N stretching band at 1205 cm^{-1} and C–S stretching band at 806 cm^{-1} [44]. These peaks infer the formation of a self-assembled monolayer of MOTBI on the copper surface. The lowering of C=N stretching band from 1600 cm^{-1} [45] to 1456 cm^{-1} and C–N stretching band from 1276 cm^{-1} [44] to 1205 cm^{-1} reveal the formation of complex between MOTBI SAM and copper surface through nitrogens. The vibration stretching band at 533 cm^{-1} is due to the copper oxide formed due to initial oxidation of copper surface during formation of SAM [39].

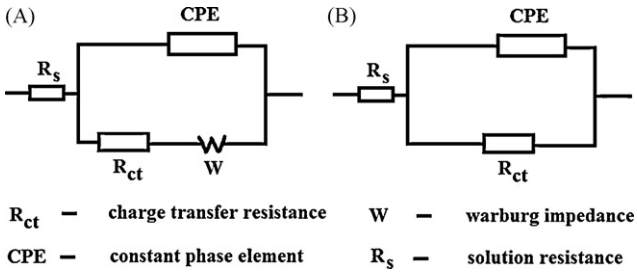

Fig. 6. Equivalent circuit used in impedance measurements of (A) bare copper electrode and (B) copper electrode covered with MOTBI SAM.

3.3. Corrosion protection of copper by MOTBI SAM

3.3.1. Electrochemical impedance studies in NaCl environment

Nyquist plots of bare copper and SAM covered copper electrodes are obtained in aqueous NaCl solution. Impedance parameters for the bare and SAM covered copper electrodes are obtained using two different equivalent circuit models [46], which are shown in Fig. 6A and B respectively. The Nyquist plots of bare copper and copper covered MOTBI SAM in NaCl solutions at different concentrations (0.02–0.20 M) are shown in Fig. 7A and B respectively and the corresponding charge-transfer resistance (R_{ct}), constant phase element (CPE) and *n* values are shown in Table 1. The small high-frequency semicircle, which is observed in the Nyquist plots for bare copper electrode in NaCl solutions is attributable to the time constant of charge-transfer resistance (R_{ct}) and the double-layer capacitance (C_{dl}) [47,48]. In the high frequency region, the electrode reaction is controlled by a charge-transfer process and the diameter of the semicircle represents the charge-transfer resistance (R_{ct}). Studies reported in the literature [49] showed that the diffusion process is controlled by diffusion of dissolved oxygen from the bulk solution to the electrode surface and the Warburg impedance, which is observed in the low frequency regions, is ascribed to diffusion of oxygen to the copper surface. The high frequency capacitive loop is so small that it is almost shielded by a straight line in the low frequency region.

The Nyquist plots of MOTBI SAM covered copper electrodes are quite different from those of bare copper electrodes. For the SAM covered copper electrode, the Warburg impedance disappeared at low frequencies, indicating that the SAM is sufficiently densely packed to prevent the diffusion of oxygen to the copper substrate and thus inhibit corrosion of copper. A large depressed semicircle is observed from high to low frequency regions in the Nyquist plots of SAM covered copper, indicating that the charge-transfer resistance becomes dominant in the corrosion process due to the presence of protective SAM on the copper surface. The impedance plots are often depressed semicircles in a practical electrode system. This phenomenon is known as the dispersing effect [50]. When the complex plane impedance contains a depressed semicircle with centre below the real axis, which is a characteristic for solid electrodes, it is often attributed to roughness and inhomogeneities of the solid surface [51]. It is also attributed to the distribution of active sites, adsorption of inhibitor molecules and formation of porous layers

Table 1
Impedance parameters of bare copper and copper covered with MOTBI SAM in NaCl environment at different concentrations (immersion period: 0.5 h; temperature: 30 °C).

S. no.	Specimen	NaCl concentration (M)	Charge-transfer resistance, R_{ct} (kΩ cm^2)	Constant phase element, CPE (μF/cm^2)	n	IE%
1	Bare copper	0.02	2.60	4.00	0.46	–
2	Copper with SAM	0.02	372.1	0.12	0.80	99.3
3	Bare copper	0.05	2.27	5.91	0.46	–
4	Copper with SAM	0.05	334.0	0.12	0.79	99.3
5	Bare copper	0.10	2.01	8.58	0.42	–
6	Copper with SAM	0.10	201.8	0.14	0.80	99.0
7	Bare copper	0.15	1.96	8.04	0.38	–
8	Copper with SAM	0.15	151.7	0.18	0.772	98.7
9	Bare copper	0.20	1.89	11.16	0.38	–
10	Copper with SAM	0.20	123.4	0.21	0.74	98.4

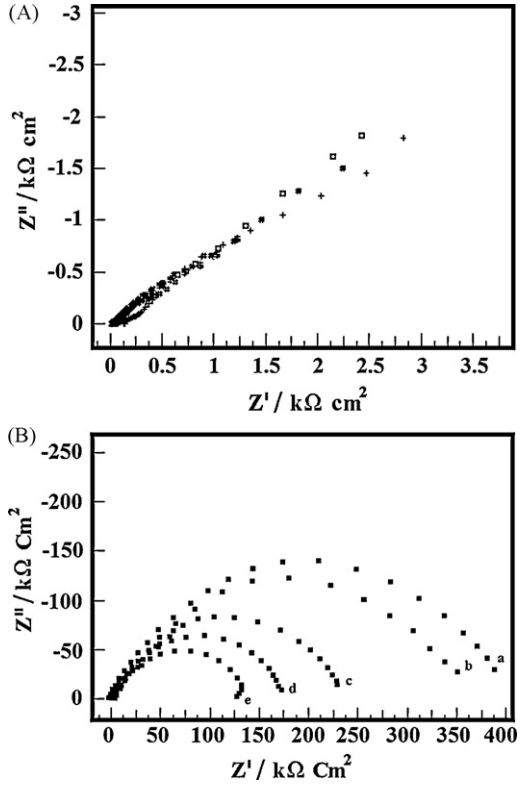

Fig. 7. (A) Nyquist plots of bare copper electrode in different concentrations of NaCl as corrosive environment. +, 0.02 M; ◘, 0.05 M; #, 0.10 M; ▞, 0.15 M; $, 0.20 M (immersion period: 0.5 h; temperature: 30 °C). (B) Nyquist plots of MOTBI SAM covered copper electrode in different concentrations of NaCl. a, 0.02 M; b, 0.05 M; c, 0.10 M; d, 0.15 M; e, 0.20 M (immersion period: 0.5 h; temperature: 30 °C).

[52]. Due to the fact that the double-layer does not behave as an ideal capacitor in the presence of the dispersing effect, a constant phase element (CPE) is often used as a substitute for the capacitor in the equivalent circuit to fit the impedance behavior of the electrical double-layer more accurately [50]. CPE can thus be regarded as a non-ideal capacitance [53]. The CPE is a special element, whose value is a function of the angular frequency, ω, and whose phase is independent of the frequency. Its admittance and impedance are, respectively, expressed as

$$Y_{CPE} = Y_0(j\omega)^n \quad (1)$$

$$Z_{CPE} = \frac{1}{Y_0(j\omega)^{-n}} \quad (2)$$

where Y_0 is the magnitude of the CPE, ω is the angular frequency and n is the exponential term of the CPE [50]. The n value is used to account for the roughness of the electrode. The lower the value of n, the rougher the electrode surface, and a smaller R_{ct} value corresponds to a higher corrosion rate. The value of n is also related to the inherent physical and chemical heterogeneous nature of the solid surface [54], the presence of a porous corrosion product layer [55], non-uniform distribution of current density on the surface [56], etc.

All the Nyquist plots obtained in the present study are characterized by single time constant. Charge-transfer resistance (R_{ct}) and the non-ideal capacitance (CPE) are the two important parameters related to corrosion processes at the metal/solution interface. The former one is directly related to the rate of corrosion reaction at the interface while the latter is related to the structure of electrical double-layer at the interface. R_{ct} value for bare copper in 0.02 M NaCl is 2.60 kΩ cm^2, which increased to 372.1 kΩ cm^2 for copper covered with MOTBI SAM in the same environment. The CPE value at the copper/0.02 M NaCl interface is found to decrease from 4.00 μF/cm^2 in the case of bare copper to a very small value such as 0.12 μF/cm^2 in the case of copper surface covered with SAM. This is because the water molecules in the electrical double-layer are replaced almost completely by the organic molecules having a very low dielectric constant [5]. In NaCl solutions the value of n has considerably increased in presence of SAM on copper surface. For example in 0.02 M NaCl environment, the value of n increased from 0.46 to 0.80. These results indicate that the copper surface has become smoother due to formation of a non-porous and dense monolayer of MOTBI. Inhibition efficiencies are found to be in the

Table 2
Impedance parameters of bare copper and copper covered with MOTBI SAM in 0.02 M NaCl environment at different immersion periods (temperature: 30 °C).

S. no.	Specimen	Immersion time (h)	Charge-transfer resistance, R_{ct} (kΩ cm^2)	Constant phase element, CPE (μF/cm^2)	n	IE%
1	Bare copper	0.5	2.60	4.00	0.46	–
2	Copper with SAM	0.5	372.1	0.12	0.80	99.3
3	Bare copper	6	2.58	6.81	0.46	–
4	Copper with SAM	6	223.7	0.18	0.76	98.8
5	Bare copper	12	2.46	7.30	0.45	–
6	Copper with SAM	12	199.9	0.18	0.76	98.7
7	Bare copper	24	2.42	8.93	0.45	–
8	Copper with SAM	24	164.8	0.27	0.74	98.5

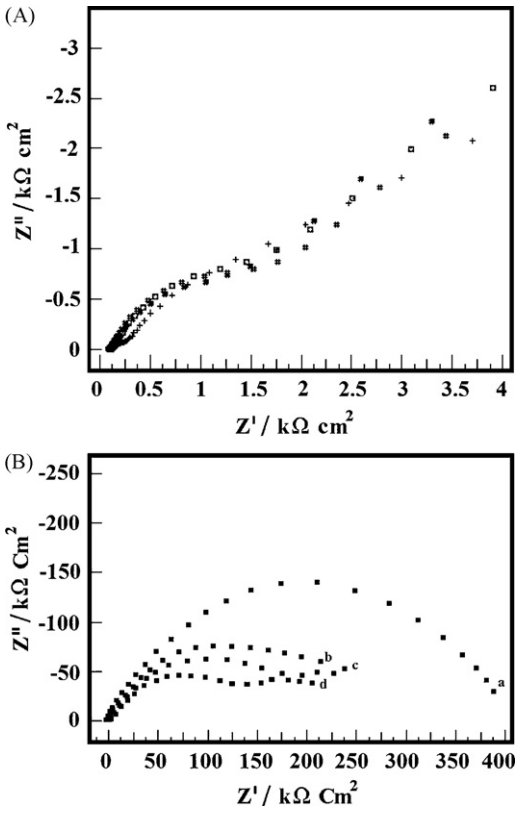

Fig. 8. (A) Nyquist plots of bare copper electrode in 0.02 M NaCl corrosive environment at different immersion periods. +, 0.5 h; ■, 6 h; #, 12 h; ##, 24 h (temperature: 30 °C). (B) Nyquist plots of MOTBI SAM covered copper electrode in 0.02 M NaCl at different immersion periods. a, 0.5 h; b, 6 h; c, 12 h; d, 24 h (temperature: 30 °C).

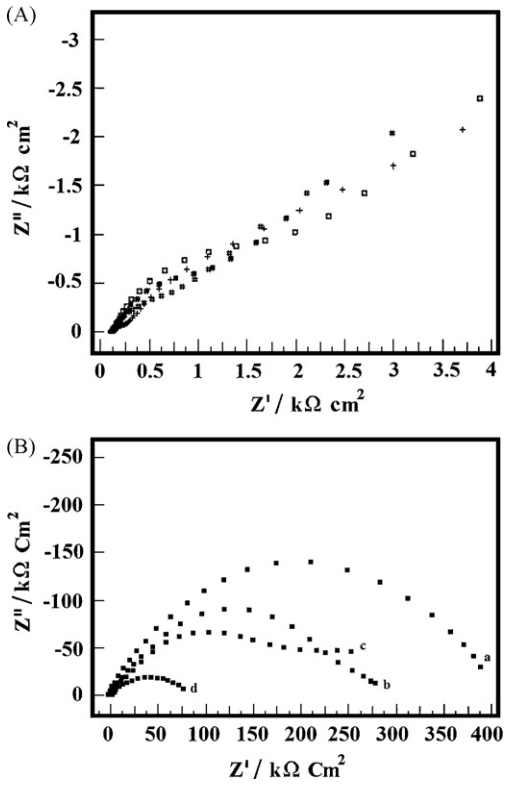

Fig. 9. (A) Nyquist plots of bare copper electrode in 0.02 M NaCl at different temperatures. +, 30 °C; ■, 40 °C; #, 50 °C; ##, 60 °C (immersion period: 0.5 h). (B) Nyquist plots of MOTBI SAM covered copper electrode in 0.02 M NaCl at different temperatures. a, 30 °C; b, 40 °C; c, 50 °C; d, 60 °C (immersion period: 0.5 h).

range of 99.3–98.4% in NaCl environment within the concentration range studied.

The Nyquist plots of bare copper and SAM covered copper in 0.02 M NaCl solutions at different immersion periods (0.5–24 h) and at a constant temperature of 30 °C are shown in Fig. 8A and B respectively and the corresponding charge-transfer resistance (R_{ct}), constant phase element (CPE) and n values are shown in Table 2. With increase in immersion time, R_{ct} values decreased slightly, CPE values increased slightly and n values decreased slightly due to long exposure of SAM to the corrosive ions. The slight increase in CPE is due to increase in the specific area caused by the presence of corrosion products on the metallic surface with time [57]. The values of n at various immersion periods are close to each other, which infer that the homogeneity of the monolayer is maintained during the immersion period studied. Inhibition efficiencies are found to be in the range of 99.3–98.5% in 0.02 M NaCl environment within the immersion period range studied. The Nyquist plots of bare copper and SAM covered copper in 0.02 M NaCl solutions at different temperatures (30–60 °C) and at a constant immersion period of 0.5 h are shown in Fig. 9A and B respectively and the corresponding charge-transfer resistance (R_{ct}), constant phase element (CPE) and n values are shown in Table 3. R_{ct} values are found to decrease for both bare copper and SAM covered copper with increase in temperature. Increase in temperature leads to an increase in corrosion rate in the absence and presence of corrosion inhibitors [58]. Slight increase in CPE values and decrease in n values are observed. These observations can be attributed to the slight changes in the monolayer present on the surface, making it slightly porous and inhomogeneous. Nevertheless, the protective nature of the SAM is clearly inferred by the high inhibition efficiencies even at high temperatures. The inhibition efficiencies are found to be in the range of 99.3–97.1% in 0.02 M NaCl environment within the temperature range studied. It is evident from this result that the corrosion protection of SAM is excellent within the temperature range studied.

Thus, all the observations in the impedance studies indicate that there is formation of a nonporous and highly protective SAM on copper surface, which effectively protects the metal surface from

Table 3
Impedance parameters of bare copper and copper covered with MOTBI SAM in 0.02 M NaCl environment at different temperatures (immersion period: 0.5 h).

S. no.	Specimen	Temperature (°C)	Charge-transfer resistance, R_{ct} (kΩ cm²)	Constant phase element, CPE (μF/cm²)	n	IE%
1	Bare copper	30	2.60	4.00	0.46	–
2	Copper with SAM	30	372.1	0.12	0.80	99.3
3	Bare copper	40	2.50	5.79	0.45	–
4	Copper with SAM	40	217.6	0.14	0.79	98.8
5	Bare copper	50	2.44	7.71	0.45	–
6	Copper with SAM	50	193.5	0.18	0.76	98.7
7	Bare copper	60	2.40	8.84	0.41	–
8	Copper with SAM	60	83.5	0.43	0.65	97.1

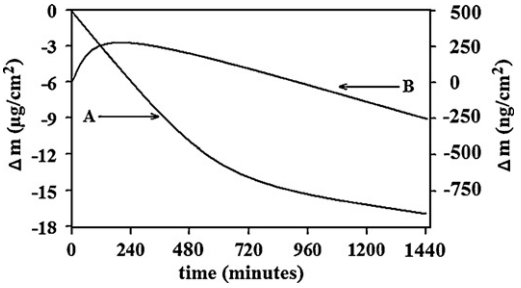

Fig. 10. Mass change vs. time curve on copper quartz crystal in corrosive environment. 0.02 M NaCl. (A) Bare copper (left side *Y*-axis scale); (B) SAM covered copper (right side *Y*-axis scale).

corrosion in aggressive environment, even at long immersion periods of 24 h and temperatures up to 60 °C.

3.3.2. Results of studies using electrochemical quartz crystal nanobalance

EQCN measurements are carried out with the bare copper quartz crystal as well as with the SAM covered copper quartz crystal in the corrosive environment namely 0.02 M NaCl and the mass change vs. time curves are shown in Fig. 10. After 24 h of immersion, mass change of the bare copper is found to be −17 μg/cm^2 while the mass change of the SAM covered copper quartz crystal is only −0.3 μg/cm^2. This result further supports the protective nature of MOTBI SAM.

3.3.3. Potentiodynamic polarization studies

Potentiodynamic polarization curves for bare copper and copper covered with MOTBI SAM are obtained in NaCl solutions over a concentration range of 0.02–0.20 M after an immersion period of 0.5 h and shown in Fig. 11A and B respectively. The corrosion current densities (i_{corr}) are determined from the polarization curves by the Tafel extrapolation method. SAM formed on the copper surface acts as a barrier to the diffusion of oxygen molecules from the solution to the copper surface, thereby resisting the transfer of oxygen to the cathodic sites of the copper surface. Compared with the bare copper, lower i_{corr} values are obtained for SAM covered copper in NaCl solutions as shown in Table 4. With increase in NaCl concentration, i_{corr} values increased for both bare copper and copper covered SAM. The corrosion potential (E_{corr}) of the copper electrode shifted towards more negative side after the deposition of SAM on copper surface. The cathodic Tafel slope is shifted to a great extent in presence of the MOTBI SAM on the copper surface. For example in 0.02 M NaCl, the cathodic Tafel slope (b_c) is shifted from −433 mV/dec to −32 mV/dec in the presence of MOTBI SAM on the copper surface. It may be inferred that MOTBI SAM on copper surface has retarded the cathodic reaction of the corrosion process.

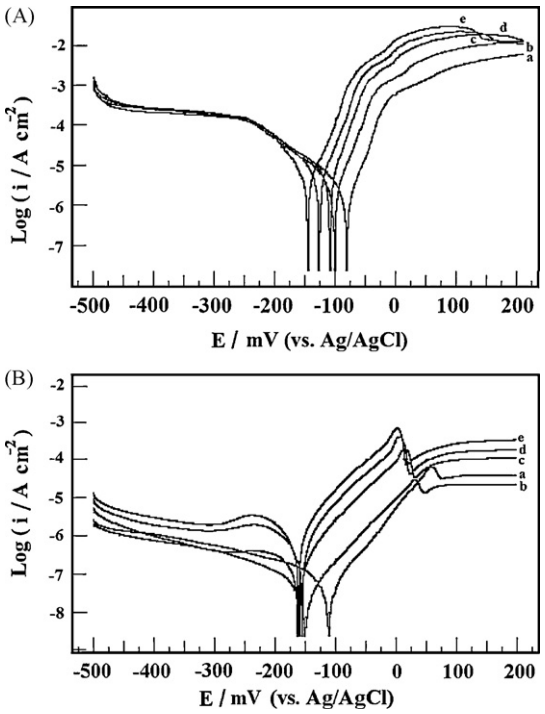

Fig. 11. Potentiodynamic polarization curves of (A) bare copper electrode and (B) MOTBI SAM covered copper electrode in different concentrations of NaCl. a, 0.02 M; b, 0.05 M; c, 0.10 M; d, 0.15 M; e, 0.20 M (immersion period: 0.5 h; temperature: 30 °C).

3.3.4. Results of X-ray photoelectron spectroscopic studies

In the XPS survey spectrum of bare copper immersed in 0.02 M NaCl environment for 3 days, Cu 2p$_{3/2}$, Cu 2p$_{1/2}$ and O 1s peaks are detected, along with Cl 2p peak at 199.8 eV. The computer deconvolution spectrum for Cl 2p is shown in Fig. 12. This peak is due to the formation of $CuCl_2$ on copper surface. The XPS spectrum of copper covered with MOTBI SAM immersed in 0.02 M NaCl environment for 3 days shows peaks corresponding to Cu 2p$_{3/2}$, Cu 2p$_{1/2}$, O 1s, C 1s, N 1s and S 2p. Cl 2p peak is not found. The computer deconvolution spectra for copper, oxygen, carbon, nitrogen and sulfur are shown in Fig. 13A–E respectively. A very small increase in intensity of O 1s peak is observed. However, no change is observed in the intensities of Cu 2p, C 1s, N 1s and S 2p peaks. It is thus evident from the XPS spectra that the MOTBI SAM offers good protection to copper surface from corrosion in the environment studied.

3.3.5. Results of weight-loss studies

Results of weight-loss studies for an immersion period of 3 days in 0.02 M NaCl environment, showed a corrosion rate of

Table 4
Corrosion parameters obtained by potentiodynamic polarization studies of bare copper and copper covered with MOTBI SAM in NaCl environment at different concentrations (immersion period: 0.5 h; temperature: 30 °C).

S. no.	Specimen	NaCl concentration (M)	E_{corr} (mV)	i_{corr} (μA/cm^2)	b_a (mV/decade)	b_c (mV/decade)	IE%
1	Bare copper	0.02	−83.4	11.9	80	−433	–
2	Copper with SAM	0.02	−111.1	0.01	28	−32	99.91
3	Bare copper	0.05	−99.6	14.1	64	−442	–
4	Copper with SAM	0.05	−149.3	0.02	52	−66	99.85
5	Bare copper	0.10	−108.6	16.0	52	−456	–
6	Copper with SAM	0.10	−161.2	0.13	46	−111	99.18
7	Bare copper	0.15	−128.7	17.2	56	−419	–
8	Copper with SAM	0.15	−153.9	0.67	52	−158	96.10
9	Bare copper	0.20	−147.0	19.6	60	−427	–
10	Copper with SAM	0.20	−162.0	1.21	55	−147	93.82

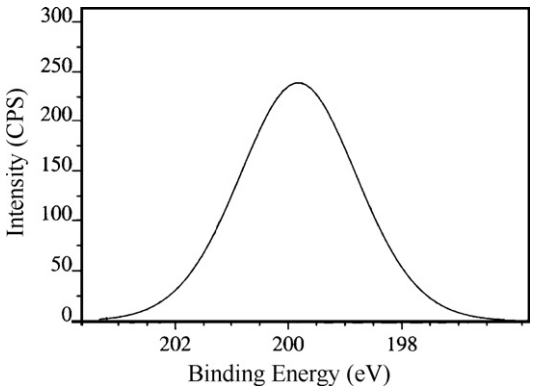

Fig. 12. XPS deconvolution spectrum of Cl 2p present on the surface of the bare copper after immersion in 0.02 M NaCl solution for a period of 3 days.

0.0641 mm/year for bare copper and only 0.0004 mm/year for copper covered with MOTBI SAM. The relative standard error in corrosion rate determinations is of the order of 2% or less [59]. An inhibition efficiency of 99.4% is obtained from weight-loss studies. These results infer that the corrosion protection ability of the MOTBI SAM is quite good even after an immersion period of 3 days in the corrosive environment. The inhibition efficiency obtained from weight-loss studies is in good agreement with the values obtained from impedance studies and polarization studies though the immersion period is different in each of the methods.

3.3.6. Results of quantum chemical calculations

It has been reported that the higher the HOMO energy level of the inhibitor, the greater is the ease of offering electrons to the unoccupied d orbital of metallic copper and the greater the inhibition efficiency [60]. It is inferred that the more negative the atomic charges of the adsorbed centre, the more easily the atom donates its electrons to the unoccupied orbital of the metal [61]. It has also been reported that inhibitors can form coordination bonds between the unshared electron pair of the N atom, π electrons of aromatic ring and the unoccupied d electron orbital of the metal [62]. The larger the negative charge of the N atom, the better is the action as an electron donor. Table 5 shows the energy of the highest occupied molecular orbital (HOMO), energy of the lowest unoccupied molecular orbital (LUMO), the energy difference between LUMO and HOMO, the electron density for atoms in the ring and the total ring electron density for the MOTBI molecule. Thus, the greater inhibition efficiency of MOTBI for copper corrosion in NaCl solution can be attributed to the higher HOMO energy, lower energy gap between LUMO and HOMO and a very high negative total ring charge of the MOTBI molecule. The higher negative charge on N atoms suggests the possibility of complex formation between Cu^+ ions and MOTBI through nitrogens.

3.4. Mechanistic aspects of corrosion protection by SAM

In the absence of SAM anodic dissolution of copper in chloride environment proceeds via a two-step oxidation process [33].

$$Cu + Cl^- \rightarrow CuCl + e^- \quad (3)$$

$$CuCl + Cl^- \rightarrow CuCl_2^- \quad (4)$$

The CuCl has poor adhesion and is unable to protect the copper surface, and transforms into the soluble cuprous chloride complex, $CuCl_2^-$ [63]. In neutral environment like NaCl, the presence of oxygen enhances the cathodic reaction due to oxygen reduction [14].

$$O_2 + 2H_2O + 4e^- \rightarrow 4OH^- \quad (5)$$

A plausible mechanism for corrosion protection of copper by MOTBI SAM is discussed hereunder. The structure of the MOTBI molecule is already shown in Fig. 1. This molecule can exist in different resonance structures as shown in Fig. 14. This molecule gets chemisorbed on the surface of copper and forms a chelate with Cu^+ ions already existing on the copper surface due to initial corrosion of copper. The lone pairs of electrons on the two nitrogens, the π electrons of the benzene ring, the lone pair of electrons on

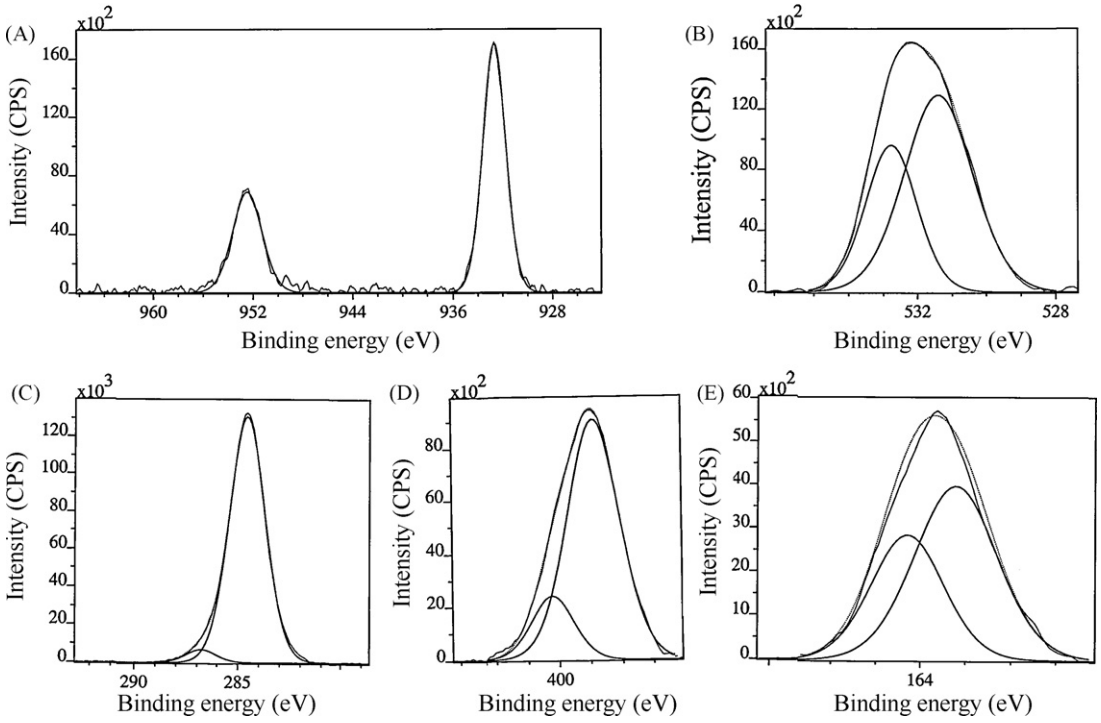

Fig. 13. XPS deconvolution spectra of different elements present on the copper covered with MOTBI SAM after immersion in 0.02 M NaCl solution for a period of 3 days: A, Cu 2p; B, O 1s; C, C 1s; D, N 1s; E, S 2p.

Table 5
Quantum chemical parameters for MOTBI calculated by AM1 method.

E_{HOMO} (eV)	E_{LUMO} (eV)	ΔE (eV)	Net atomic charges											
			C(1)	N(2)	C(3)	C(4)	N(5)	H(6)	C(7)	C(8)	C(9)	C(10)	S(11)	Ring charge
−9.66	−1.69	7.97	−0.13	−0.19	−0.01	−0.04	−0.36	0.33	−0.20	0.06	−0.19	−0.15	0.29	−1.23

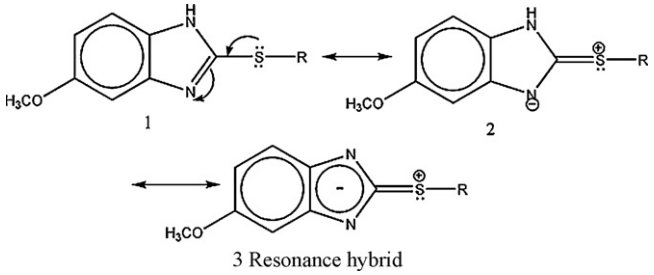

Fig. 14. Resonance structures of the MOTBI molecule (–R = –$(CH_2)_{17}$–CH_3).

the oxygen of the MeO group, participation of nonbonded electrons of the sulfur in resonance due to +mesomeric effect of sulfur contribute to a large negative value of the total ring charge. Zhang et al. [64] found that in comparison to imidazole, 1-*n*-undecyl-imidazole (UDIM) exhibited better corrosion inhibition efficiency for copper in 0.5 M HCl and attributed the same to its relatively larger negative ring charge of −0.5309. In comparison to UDIM, MOTBI has a much higher negative ring charge of −1.23. Such a very large negative total ring charge favors the formation of a coordinate linkage between MOTBI and Cu^+ ions available on copper surface through the two nitrogens present in the imidazole ring. Surface enhanced Raman spectral studies of the chemisorbed imidazole molecules on the copper surface [65] inferred that the imidazole molecules are oriented parallel to the copper surface. The MOTBI molecules, which are essentially derived from the imidazole moiety, are considered to be oriented parallel to the copper surface. In such an orientation, the [Cu^+-MOTBI] complexation may lead to the formation of a polymeric network on the copper surface as shown in Fig. 15. It may be noted that Cu^+ is known to form bidentate complexes. Besides the strong coordinate linkages between Cu^+ and N, there are non-covalent interactions namely π-stack interactions between benzene rings and the van der Waals interactions between the long alkyl chains. Thus, there is formation of a [Cu^+-MOTBI] polymeric complex, which is highly protective in nature.

Tan et al. [32] reported that the molecular thicknesses of all the benzene thiol films on copper are less than 2 nm and interpreted that the surface layer is restricted to a chemisorbed monolayer.

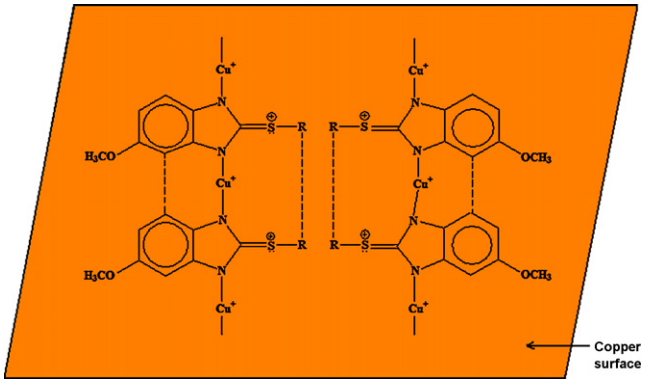

Fig. 15. Schematic of formation of a protective SAM by MOTBI on copper surface. Complex formation between Cu^+ ions on copper surface and MOTBI molecules oriented parallel to copper surface, is shown. – – – lines indicate π-stack and van der Waals interactions.

Some authors [66,67] have reported the film thickness of around 2 nm for the alkanethiol surface films. They interpreted that the intermolecular interaction between the alkyl chains is responsible for the formation of ordered monolayer but not a multilayer. Quan et al. [68] prepared self-assembled monolayers of schiff base on copper surface and immersed in a solution of 1-dodecanethiol to improve the corrosion protection of copper. They found that the thiol molecules subsequently adsorbed, were bonded directly on copper surface rather than physisorbed on the previous schiff base layer. They reported the formation of self-assembled monolayer but not multilayer. Taneichi et al. [37] modified the self-assembled monolayers of 11-mercapto-1-undecanol using octyl and octadecyl isocyanates on copper surface and established their corrosion protection efficiency. They interpreted the inhibited films in terms of self-assembled monolayers. Hao et al. [69] studied the corrosion protection ability of self-assembled monolayer of phytic acid on cupronickel B30 and showed that the adsorption mechanism of phytic acid is typical of chemisorption following Langmuir's adsorption isotherm. They interpreted that the corrosion protection efficiency is because of the formation of self-assembled monolayer of phytic acid on the metal surface due to complexation between Cu^+ ions and phytic acid. Alagta et al. [70] studied the corrosion protection properties of self-assembled monolayers of hydroxamic acids with different alkyl lengths formed on copper surface and carbon steel. They demonstrated from the surface morphology studies by atomic force microscope [71] that there is formation of self-assembled monolayer only. In the light of the above results and interpretations reported in the literature it is proposed that in the case of the present study of self-assembly of 5-methoxy-2-(octadecylthio)benzimidazole on copper, there is formation of a chemisorbed monolayer of polymeric [Cu^+-MOTBI] complex.

4. Conclusion

It is necessary to establish the optimum conditions for the formation of protective self-assembled monolayers of organic molecules on metal surfaces. The optimum conditions for the formation of protective SAM of 5-methoxy-2-(octadecylthio)benzimidazole on copper surface are (i) etching of copper surface in 7N nitric acid for 30 s, (ii) methanol solvent, (iii) 10 mM concentration of MOTBI and (iv) immersion time of 24 h. The SAM formed by MOTBI on copper surface offers excellent corrosion protection of copper in NaCl solution within the concentration range studied, i.e., up to 0.20 M at the ambient temperature of 30 °C. The MOTBI SAM offers good inhibition up to a temperature of 60 °C in 0.02 M NaCl solution. The inhibition efficiencies obtained from weight-loss studies, electrochemical impedance studies and polarization studies are in good agreement with each other. The nature of the protective monolayer formed on the copper surface plays a key role in the corrosion inhibition. The MOTBI molecules gets chemisorbed on copper surface and form a polymeric coordination complex with Cu^+ ions through nitrogen atoms in the ring.

Acknowledgements

One of the authors, Mr. Md. Yakub Iqbal is thankful to the National Institute of Technology Warangal, for providing

the institute fellowship under the Technical Education Quality Improvement Programme of the Government of India.

References

[1] Minges, L. Merrill, Electronic Materials Handbook, vol. 1: Packaging, ASM International, Materials Park, OH, 1989.
[2] H.M. Ho, W. Lam, S. Stoukatch, P. Ratchev, C.J. Vath III, E. Beyne, Microelectron. Reliab. 43 (2003) 913.
[3] C.M. Whelan, M. Kinsella, L. Carbonell, H.M. Ho, K. Maex, Microelectron. Eng. 70 (2003) 551.
[4] C. Liu, D.A. Hutt, IEEE Trans. Compon. Packag. Technol. 29 (2006) 512.
[5] C.T. Wang, S.H. Chen, H.Y. Ma, L. Hua, N.X. Wang, J. Serb. Chem. Soc. 67 (10) (2002) 685.
[6] P.E. Laibinis, G.M. Whitesides, J. Am. Chem. Soc. 114 (1992) 9022.
[7] Y.Q. Feng, W.K. Teo, K.S. Siow, Z.Q. Gao, K.L. Tan, A.K. Hsieh, J. Electrochem. Soc. 144 (1997) 55.
[8] Y. Yamamoto, H. Nishihara, K. Aramaki, J. Electrochem. Soc. 140 (1993) 436.
[9] Z. Quan, X. Wu, S. Chen, S. Zhao, H. Ma, Corrosion 57 (2001) 195.
[10] Z. Quan, S. Chen, X. Cui, Y. Li, Corrosion 58 (2002) 248.
[11] D.H. Gracias, U.S. Patent, 6,858,527, February 22, 2005.
[12] M.M. Antonijevic, M.B. Petrovic, Int. J. Electrochem. Sci. 3 (2008) 1.
[13] E. Stupnisek-Lisac, A. Gazivoda, M. Madzarac, Electrochim. Acta 47 (2002) 4189.
[14] H. Otmacic, E. Stupnisek-Lisac, Electrochim. Acta 48 (2003) 985.
[15] W.-J. Lee, Mater. Sci. Eng. A 348 (2003) 217.
[16] E. Stupnisek-Lisac, V. Cinotti, D. Reichenbach, J. Appl. Electrochem. 29 (1999) 117.
[17] D.-Q. Zhang, L.-X. Gao, G.-D. Zhou, J. Appl. Electrochem. 33 (2003) 361.
[18] D.-Q. Zhang, L.-X. Gao, G.-D. Zhou, Corros. Sci. 46 (2004) 3031.
[19] L. Larabi, O. Benali, S.M. Mekelleche, Y. Harek, Appl. Surf. Sci. 25 (2006) 1371.
[20] R. Subramanian, V. Lakshminarayanan, Corros. Sci. 44 (2002) 535.
[21] G. Xue, X.-y. Huang, J. Ding, J. Chem. Soc., Faraday Trans. 87 (1991) 1229.
[22] G. Xue, X.-y. Huang, J. Dong, J. Zhang, J. Electroanal. Chem. 310 (1991) 139.
[23] K.T. Carron, M.L. Lewis, J. Dong, J. Ding, G. Xue, Y. Chen, J. Mater. Sci. 28 (1993) 4099.
[24] V. Rajeswar Rao, V. Ravi Kumar, Ind. J. Chem. Sect. B 41B (2002) 415.
[25] M. Ishibashi, M. Itoh, H. Nishihara, K. Aramaki, Electrochim. Acta 41 (1996) 241.
[26] H. Tavakoli, T. Shahrabi, M.G. Hosseini, Mater. Chem. Phys. 109 (2008) 281.
[27] J. Telegdi, A. Shaban, E. Kalman, Electrochim. Acta 45 (2000) 3639.
[28] G. Sauerbrey, Z. Phys. 155 (1959) 206.
[29] J.B. Brzoska, N. Shahidzadeh, F. Rondelez, Nature 360 (1992) 719.
[30] M.M. Sung, K. Sung, C.G. Kim, S.S. Lee, Y. Kim, J. Phys. Chem. B 104 (2000) 2273.
[31] J. Telegdi, T. Rigo, E. Kalman, Corros. Eng. Sci. Technol. 39 (2004) 65.
[32] Y.S. Tan, M.P. Srinivasan, S.O. Pehkonen, S.Y.M. Chooi, Corros. Sci. 48 (2006) 840.
[33] G.P. Cicileo, B.M. Rosales, F.E. Varela, J.R. Vilche, Corros. Sci. 41 (1999) 1359.
[34] X.R. Ye, X.Q. Xin, J.J. Zhu, Z.L. Xue, Appl. Surf. Sci. 135 (1998) 307.
[35] G. Petkova, E. Sokolova, S. Raicheva, P. Ivanov, J. Appl. Electrochem. 28 (1998) 1067.
[36] D.A. Hutt, C. Liu, Appl. Surf. Sci. 252 (2005) 400.
[37] D. Taneichi, R. Haneda, K. Aramaki, Corros. Sci. 43 (2001) 1589.
[38] A.M. Beccaria, C. Bertolotto, Electrochim. Acta 42 (1997) 1361.
[39] G. Papadimitropoulos, N. Vourdas, V.Em. Vamvakas, D. Davazoglou, J. Phys.: Conf. Ser. 10 (2005) 182.
[40] Z. Mekhalif, G. Fonder, F. Laffineur, J. Delhalle, J. Electroanal. Chem. 621 (2008) 245.
[41] S. Yoshida, H. Ishida, Appl. Surf. Sci. 89 (1995) 39.
[42] P.E. Laibinis, G.M. Whitesides, D.L. Allara, Y.-T. Tao, A.N. Parikh, R.G. Nuzzo, J. Am. Chem. Soc. 113 (1991) 7152.
[43] R.M. Silverstein, F.x. Webster, Spectroscopic Identification of Organic Compounds, 6th Wiley Student edition, Wiley India (P) Ltd., New Delhi, 2007, p. 82.
[44] A. Lalitha, S. Ramesh, S. Rajeswari, Electrochim. Acta 51 (2005) 47.
[45] H. Baba, T. Kodama, K. Mori, H. Hirahara, Corros. Sci. 39 (1997) 555.
[46] G. Li, H. Ma, Y. Jiao, S. Chen, J. Serb. Chem. Soc. 69 (10) (2004) 791.
[47] O.E. Barcia, O.R. Mattos, N. Pebere, B. Tribollet, J. Electrochem. Soc. 140 (1993) 2825.
[48] Y. Feng, W.K. Teo, K.S. Siow, K.L. Tan, A.K. Hsieh, Corros. Sci. 38 (1996) 369.
[49] H. Ma, S. Chen, L. Niu, S. Zhao, S. Li, D. Li, J. Appl. Electrochem. 32 (2002) 65.
[50] X. Wu, H. Ma, S. Chen, Z. Xu, A. Sui, J. Electrochem. Soc. 146 (1999) 1847.
[51] K. Juttner, Electrochim. Acta 35 (1990) 1501.
[52] A.A. Ec Hosary, R.M. Saleh, A.M. Shams El Din, Corros. Sci. 12 (1972) 897.
[53] W. Scheider, J. Phys. Chem. 79 (1975) 127.
[54] E.Mc. Cafferty, Corros. Sci. 39 (1997) 243.
[55] M. Touzet, M. Cid, M. Puiggali, M.C. Petit, Corros. Sci. 34 (1993) 1187.
[56] D.D. Macdonald, M.C.H. Mckubre, in: J.O'M. Bockris, B.E. Conwey, R.E. White (Eds.), Modern Aspects of Electrochemistry, Plenum Press, New York, 1982, p. 61.
[57] A. Bonnel, F. Dabosi, C. Deslovis, M. Duprat, M. Keddam, B. Tribollet, J. Electrochem. Soc. 130 (1983) 753.
[58] A. Dafali, B. Hammouti, R. Touzani, S. Kertit, A. Ramdani, K.EI Kacemi, Anti-Corros. Methods Mater. 49 (2) (2002) 96.
[59] R.A. Freeman, D.C. Silverman, Corrosion 48 (1992) 463.
[60] C. Ogretir, B. Mihci, G. Bereket, J. Mol. Struct.: Theochem. 488 (1999) 223.
[61] C.T. Wang, S.H. Chen, H.Y. Ma, C.S. Qi, J. Appl. Electrochem. 33 (2003) 179.
[62] D. Wang, S. Li, Y. Ying, M. Wang, H. Xiao, Z. Chen, Corros. Sci. 41 (1999) 1911.
[63] C.W. Yan, H.C. Lin, C.N. Cao, Electrochim. Acta 45 (2000) 2815.
[64] D.-Q. Zhang, L.-X. Gao, G.-D. Zhou, K.Y. Lee, J. Appl. Electrochem. 38 (2008) 71.
[65] D. Thierry, C. Leygraf, J. Electrochem. Soc. 133 (1986) 2236.
[66] Y.-W. Chang, C. Ukiwe, D.Y. Kwok, Colloids Surf. A: Physicochem. Eng. Aspects 260 (2005) 255.
[67] T. Diem, W. Fabianowski, R. Jaccodine, R. Rodowski, Thin Solid Films 265 (1995) 71.
[68] Z. Quan, S. Chen, Y. Li, X. Cui, Corros. Sci. 44 (2002) 703.
[69] C. Hao, R.-H. Yin, Z.-Y. Wan, Q.-J. Xu, G.-D. Zhou, Corros. Sci. 50 (2008) 3527.
[70] A. Alagta, I. Felhosi, I. Bertoti, E. Kalman, Corros. Sci. 50 (2008) 1644.
[71] J. Telegdi, T. Rigo, E. Kalman, J. Electroanal. Chem. 582 (2005) 191.